



# **Catheter Angiography, MR Angiography, and MR Perfusion in Posterior Reversible Encephalopathy Syndrome**

W.S. Bartynski and J.F. Boardman

*AJNR Am J Neuroradiol* 2008, 29 (3) 447-455

doi: <https://doi.org/10.3174/ajnr.A0839>

<http://www.ajnr.org/content/29/3/447>

This information is current as  
of July 2, 2025.

ORIGINAL  
RESEARCH

W.S. Bartynski  
J.F. Boardman



# Catheter Angiography, MR Angiography, and MR Perfusion in Posterior Reversible Encephalopathy Syndrome

**BACKGROUND AND PURPOSE:** The cause of posterior reversible encephalopathy syndrome (PRES) is unknown. Two primary hypotheses exist: 1) hypertension exceeding auto-regulatory limits leading to forced hyper-perfusion and 2) vasoconstriction and hypo-perfusion leading to ischemia with resultant edema. The purpose of this study was to evaluate the catheter angiography (CA), MR angiography (MRA), and MR perfusion (MRP) features in PRES in order to render further insight into its mechanism of origin.

**MATERIALS AND METHODS:** In 47 patients with PRES, 9 CAs and 43 MRAs were evaluated for evidence of vasculopathy (vasoconstriction and vasodilation), and 15 MRP studies were evaluated for altered relative cerebral blood volume (rCBV) in PRES lesions and regions. Visualization of vessels on MRA and toxicity blood pressures were compared with the extent of hemispheric vasogenic edema.

**RESULTS:** Vasculopathy was present in 8 of 9 patients on CA (direct correlation to MRA in 3/6 patients). At MRA, moderate to severe vessel irregularity consistent with vasoconstriction and vasodilation was present in 30 of 43 patients and vessel pruning or irregularity in 7 patients, with follow-up MRA demonstrating reversal of vasoconstriction or vasodilation in 9 of 11 patients. Vasogenic edema was less in patients with hypertension compared with patients who were normotensive. Preserved normal length of the posterior cerebral artery (PCA) was commonly seen in patients with severe hypertension despite diffuse or focal vasoconstriction or vasodilation. In these patients, lengthier visualization of the distal PCA correlated with a lower grade of hemispheric edema ( $P = .002$ ). Cortical rCBV was significantly reduced in 51 of 59 PRES lesions and regions compared with a healthy reference cortex (average 61% of reference cortex) with mild decrease in the remainder.

**CONCLUSION:** Vasculopathy was a common finding on CA and MRA in our patients with PRES, and MRP demonstrated reduced cortical rCBV in PRES lesions. Vasogenic edema was reduced in patients with hypertension, and superior distal PCA visualization correlated with reduced hemispheric edema in patients with PRES and severe hypertension.

Neurotoxicity with development of posterior reversible encephalopathy syndrome (PRES) is commonly seen in association with cyclosporine and FK-506 immune suppression after transplantation (allogeneic bone marrow transplantation [allo-BMT], solid organ transplantation); preeclampsia and eclampsia; infection, sepsis, and shock; nonspecific medical renal disease; and in autoimmune conditions as well as after high-dose chemotherapy.<sup>1-13</sup> The mechanism behind the development of PRES is yet unproved. Two broad theories have generally been considered.

Severe hypertension with autoregulatory failure and hyperperfusion is often cited as the underlying mechanism. Alternatively, vasospasm has been demonstrated (catheter angiography [CA], MR angiography [MRA]), decreased cerebral blood flow noted (MR perfusion [MRP], single-photon emission CT [SPECT]) and the imaging appearance typically resembles a watershed distribution suggesting a mechanism related to brain hypoperfusion.<sup>1-3,5,9,13-20</sup>

Given these opposing views, it was our opinion that parallel

observations on CA, MRA, and MRP could render further insight into the state of brain perfusion in PRES. Therefore, the purpose of this study was to retrospectively evaluate the CA, MRA, and MRP features in a large group of patients with PRES.

## Materials and Methods

We searched the radiology report data base at our institution (January 1998–October 2006) for patients in whom PRES, cyclosporine, tacrolimus, and FK-506 neurotoxicity, hypertensive encephalopathy, systemic lupus erythematosus, Wegener granulomatosis, preeclampsia and eclampsia, or scleroderma were cited on brain MR imaging. MR imaging studies were reviewed in identified patients for features consistent with PRES. Criteria included complete or partial expression of the typical PRES pattern, reversibility on follow-up imaging, or vasogenic edema as demonstrated by MR diffusion-weighted imaging (DWI).

A total of 116 patients were identified with clinical neurotoxicity and imaging features consistent with PRES (infection, sepsis, and shock, 31.4%; transplantation/cyclosporine and FK-506, 31.4%; autoimmune disease, 11.4%; postchemotherapy, 5.7%; and eclampsia or delayed eclampsia, 11.4%). The remaining cases included isolated hypertension and undetermined associations.

MRA or CA, or both, were available in 47 of these 116 patients, and in 20 of 47, MRP was also obtained. These 47 patients form the basis of this retrospective evaluation and report. The Institutional Review Board approved this retrospective study.

Inpatient and outpatient records on each patient were com-

Received February 2, 2007; accepted after revision August 13.

From the Department of Radiology, Division of Neuroradiology, University of Pittsburgh, Presbyterian University Hospital, Pittsburgh, Penn.

Please address correspondence to Walter S. Bartynski, MD, Department of Radiology, Division of Neuroradiology, University of Pittsburgh, Presbyterian University Hospital, D132, 200 Lothrop St, Pittsburgh, PA 15213; e-mail: bartynskiws@upmc.edu

Indicates article with supplemental on-line tables.

DOI 10.3174/ajnr.A0839

hensively reviewed with relevant clinical information identified including underlying cause/association, clinical presentation, imaging time point, and baseline/toxicity blood pressures (BP). Mean arterial pressures (MAP) were calculated in a standard fashion ( $\text{MAP} = 2/3 \text{ diastolic} + 1/3 \text{ systolic pressure}$ ).

### Imaging Techniques

MR imaging was performed at 1.5T (GE Healthcare, Milwaukee, Wis) including sagittal and axial T1-weighted images (TR, 600 ms; TE, min; section thickness, 5 mm; number of acquisitions, 1) fast spin-echo axial proton-density (TR, 2000–2500 ms; TE, min; section thickness, 5 mm; number of acquisitions, 1), T2-weighted (TR, 2500–3000 ms; TE, 84–102 ms; section thickness, 5 mm; number of acquisitions, 1). We obtained MRA using 3D time-of-flight (TOF) technique (TR, default; TE, min; FA, 45°; FOV, 18–22 cm; Matrix, 226 × 224; number of acquisitions, 1) with multiple overlapping slab reconstruction.

We performed MRP using dynamic susceptibility contrast MR imaging with gradient-echo echo-planar sequence during dynamic bolus contrast administration (TR, 2040 ms; TE, 60 ms; flip angle, 60°; matrix, 96 × 128; number of acquisitions, 1). Standard dose of 0.1 mmol/kg of gadolinium dimeglumine (Magnevist; Bayer HealthCare Pharmaceuticals, Wayne, NJ) or gadopentetate (ProHance; Bracco Diagnostics, Princeton, NJ) bolus injection (antecubital; 5 mL/s) was begun 10 seconds after scan initiation with a total of 40 data collection points (phases) acquired over 12 section locations.

We obtained contrast-enhanced T1-weighted images after the MRP sequence or independently with a standard dose (0.1 mmol/kg) injection using typical T1-weighted parameters, as described above. DWI (single-shot echo-planar, 10,000 ms/min/5 mm/128 [TR/TE/section/matrix]) sequence was available in most patients. In 9 patients, CA was performed in standard fashion with common carotid/vertebral injection and digital subtraction imaging acquisition.

### Imaging Assessment-Edema Grading

PRES locations were tabulated (occipital, parietal, frontal, temporo-occipital, and cerebellar). Atypical locations (brain stem, thalamus, and basal ganglia) were also noted.

MR imaging was independently graded by 2 neuroradiologists for the extent and severity of hemispheric cortex white matter edema (grade summary: 1, limited cortex white matter edema; 2, white matter cortex edema with some deep white matter extension; 3, white matter cortex edema with limited ventricle surface extension; 4, white matter cortex edema, diffuse, widely confluent, extensive ventricle contact; 5, severe white matter cortex edema, diffuse confluence, ventricle deformity) as previously described.<sup>13</sup> Graders were blinded to the patients' blood pressures and MRA findings. Grade differences were resolved by consensus.

### Vessel and Perfusion Assessment

Vascular studies (47 patients; MRA, 43; CA, 9) were independently and blindly assessed by 2 neuroradiologists with differences resolved by consensus. Studies were graded for 2 distinct features: 1) extent of distal second- and third-order branch visualization on MRA imaging studies (best assessed in the PCA branches) and 2) presence or absence of vasculopathy (vasoconstriction, vasodilation and/or string-of-bead appearance) at CA as traditionally recognized in vasospasm or arteritis as well as the features consistent with vasculopathy of the branches of the anterior cerebral artery (ACA), middle cerebral artery (MCA), and posterior cerebral artery (PCA) on MRA.

**Table 1: PCA pruning scale**

Pruning Grade	PCA Distal Visualization*
1	Normal length of the distal calcarine artery to the occipital pole
2	Moderately reduced length of the distal calcarine artery (length halfway between occipital pole and bifurcation with the parieto-occipital artery)
3	Severely reduced length of the calcarine artery (length reduced to the level of the bifurcation with the parieto-occipital artery)

**Note:**—PCA indicates posterior cerebral artery.

\* Visualized length of the calcarine artery to the tip of the occipital pole.

**Distal Branch Visualization (Pruning).** We assessed the extent of distal branch visualization on MRA studies by evaluating the distal branches of the PCA. Reduced branch visualization was characterized by PCA pruning and appeared as a distinct and separate observation from PCA spasm. PCA pruning was recognized by reduced PCA length (independent of vessel irregularity). Grade of PCA visualization was based on the length of calcarine artery visualization. PCA pruning was graded in severity on a 3-point scale and reviewed in Table 1.

MCA pruning was also noted if typically identified MCA branches demonstrated tapering and reduced visualization. The distal MCA branches were not consistently included on the 3D TOF sequence because of choice of placement of the upper margin of the slab. For this reason, observations of MCA pruning were made if available, but the MCA was not used for grading.

**Vasculopathy.** The 2 primary features of vasculopathy were tabulated separately: 1) diffuse vessel constriction or narrowing, 2) focal vessel irregularity of first-, second-, and third-order branch vessels (focal vasoconstriction, focal vasodilation, and beaded or string-of-bead appearance).<sup>21,22</sup> Diffuse vasoconstriction (narrowing or constriction) was considered present if significant diffuse vessel caliber reduction was observed in 2 or more major branch groups (ACA, MCA, and PCA). We judged focal vessel irregularity using the traditional features of vasospasm and arteritis and graded on a 4-point scale (0, normal; 1, possibly abnormal [mild vessel irregularity]; 2, moderate vessel irregularity; and 3, severe vessel irregularity).

Judgment of vessel abnormality (pruning, vasoconstriction, vasodilation, string-of-bead appearance) was referenced relative to typical benchmark normal MRA features obtained at our institution. Objective reference criteria were used to confidently grade vessel irregularity as vasculopathy: 1) a distinct change in artery caliber/morphology between 2 MRA studies, 2) correlation with catheter angiogram, 3) significant difference in vessel caliber/morphology relative to an internal patient reference, 4) age-inappropriate vessel caliber or irregularity in a young patient, and 5) obvious intrinsically abnormal ACA, MCA, and PCA branches with focal spasm and pruning or diffuse vasoconstriction.

**MR Perfusion.** We performed postprocessing using the FuncTools (GE Healthcare) workstation. Relative cerebral blood volume (rCBV) was obtained from quantification of the area under the negative enhancement integral generated. Negative enhancement integral was obtained in a standard fashion computing the area under the negative enhancement curve generated during bolus contrast arrival, with brain enhancement beginning at initiation of loss of signal intensity and continuing to the point of re-establishment of the post-enhancement baseline signal intensity. Regional rCBV region-of-interest measurements were obtained in a healthy-appearing cortex and white matter as well as areas affected with PRES as identified on MR imaging (FLAIR sequence and T2\*).

**Table 2: Presentation blood pressure and clinical associations (number of PRES patients)**

Blood Pressure	ISS	Tx	E	dE	AI	Chemo	Unk
Normotensive	8	2	—	1	—	—	—
Moderate hypertension	1	2	1	1	—	—	—
Severe hypertension	8	5	7	1	5	2	3

**Note:**—PRES indicates posterior reversible encephalopathy syndrome; ISS, infection, sepsis, and shock; Tx, transplantation; E, eclampsia; dE, delayed eclampsia; AI, autoimmune disease; Chemo, post-cancer chemotherapy; Unk, nonspecific association.

Establishing a baseline healthy cortex rCBV was challenging because of 1) altered brain blood flow in a normal-appearing brain (possibly because of intrinsic vasculopathy) and 2) potential volume averaging with cortical vessels. Computed rCBV was often mildly reduced in normal-appearing regions of the brain, in particular, the typical watershed and regions immediately adjacent to the PRES lesions.

Therefore, regions were chosen as representative of normal that had the consistently greatest rCBV in a healthy-appearing brain (typically medial frontal and parietal cortex, frontal operculum, and lateral superior temporo-occipital junction). Regions of interest were chosen to avoid visibly linear high flow from surface blood vessels that would inappropriately increase the rCBV measurements in a healthy cortex.

Normal rCBV was established averaging 10 to 20 region-of-interest maximum measurements (2–4 mL voxel) with a healthy-appearing cortex. The regions of interest were chosen to avoid visibly linear high flow from surface blood vessels that would inappropriately increase the rCBV measurements.

In the PRES lesions, 2 to 8 cortex measurements were obtained over moderate-sized focal lesions or over representative confluent regions, with careful attention not to alter measurements by extending into adjacent white matter or including dominant surface vessels. All lesion and healthy-appearing brain measurements were agreed on by consensus. Average lesion rCBV was referenced to average healthy brain rCBV obtained for that patient.

### Statistics

We evaluated the statistical significance of edema grade relative to blood pressure at toxicity using the Student *t* test and Kruskal-Wallis extension of the Wilcoxon test (PROCAPABILITY, SAS software package release 8.2; SAS Institute, Cary, NC). Observation timing effect on edema and PCA grades were tested by Kruskal-Wallis extension of the Wilcoxon test and analysis of variance. Interobserver differences for edema and PCA grades were tested by percentage agreement. The statistical significance of edema grade relative to PCA pruning and visualization grades was evaluated with the linear-by-linear association test for row and column independence, in which rows and columns have natural ordering.<sup>23</sup>

### Results

The clinical characteristics of the 47 patients with PRES on CA, MRA, and MRP are reviewed in Table 2 and On-line Table 1. There were 8 patients who were men and 39 who were women, with an average age of 44.6 years (range, 19–79 years) with clinical associations as tabulated (eclampsia or delayed eclampsia, 11; transplantation, 9 [cyclosporine and FK-506]; autoimmune disease, 5; postchemotherapy, 2; and infection, sepsis, and shock, 17). PRES was associated with drug use for hypertension (1 patient), recently developed hypertension (1

patient), and unstable hypertension or previous renal cell carcinoma (1 patient).

Presentation at toxicity included headache, change in vision, and change in mental status alone (19 patients) or followed by seizure (21 patients), with seizure only in 7 patients. In 11 patients, toxicity BP was either normal (baseline) or demonstrated minor increase in systolic pressure (average MAP, 94 mm Hg; range, 86–104 mm Hg). Other than minor fluctuations in BP as is commonly seen in patients in the intensive care unit, no significant episodes of hypertension were noted in the pretotoxicity or peritoxicity period in these patients. Toxicity BP was moderately elevated in 5 patients (average MAP, 114 mm Hg; range, 110–115 mm Hg, typically with moderate diastolic pressure elevation) and severely elevated in 31 patients (average MAP, 133 mm Hg; range, 119–177 mm Hg; significant systolic pressure elevation, diastolic pressure elevation, or both). BP in these patients was typically unstable immediately before and after toxicity and was often difficult to control after development of neurotoxicity and PRES.

Vasogenic edema was identified in typical PRES locations (occipital, 44 patients; parietal, 45 patients; frontal, 36 patients; temporooccipital junction, 22 patients; and cerebellum, 19 patients) and atypical locations (brain stem [pons, 5 patients; medulla, 2 patients; midbrain, 3 patients]); basal ganglia, 4 patients; and thalamus, 6 patients). Of 32 patients, DWI results were normal or demonstrated T2 shinedthrough in 16. In 7 patients, DWI results were normal except for a single focus of restricted diffusion (infarction, 7 patients; hemorrhage, 3 patients). Minimal stippled cortical enhancement was noted in 3 patients. Early follow-up imaging results demonstrated improvement in vasogenic edema in 12 patients with complete reversal of the PRES pattern in 19 patients. Follow-up imaging was not obtained in 16 patients, but DWI results in these patients were normal or demonstrated T2 shinedthrough.

### Vasogenic Edema and MAP

Greater hemispheric edema was present in patients who were normotensive (grade average, 2.45) with reduced edema in patients with moderate to severe hypertension (grade averages, 1.6 and 1.74, respectively). The difference between patients who were normotensive and those with severe hypertension was statistically significant ( $P = .045$ , Student *t* test). Patients with eclampsia and autoimmune disease primarily demonstrated severe hypertension and a low grade of vasogenic edema, whereas patients with infection, sepsis, and shock were commonly normotensive with more severe brain edema (Table 2 and On-line Table 1).

No statistically significant difference was detected in edema grade relative to MR imaging timing from recognized neurotoxicity. Interobserver agreement of edema grade was 60.4% before consensus resolution.

### Angiographic Features (CA and MRA)

In 46 of 47 patients, intracranial vessels could be assessed by CA (9 patients) or MRA (43 patients). In 1 patient with severe hypertension, MRA could not be assessed because of significant motion artifact. The MRA and CA features in patients with PRES are summarized in Table 3 and On-line Table 1, and in Figs 1–5.

**Table 3: Summary of MRA features and toxicity blood pressure**

	#	Overall Features			#	Focal Vessel Features		
		nl	P	DS		nl	Ir (Ir/P)	FS (FS/P)
Blood Pressure	pts				vessels			
Normotensive	10	7	3	—	30	16	12 (6)	2
Moderately hypertensive	5	2	—	3	15	4	4 (2)	7
Severely hypertensive	28	8	2	18	84	13	22 (9)	49 (5)

**Note:**—MRA indicates MR angiography; # pts indicates number of patients; nl, normal; P, pruned; DS, diffuse vasoconstriction; # vessels, number of vessels; Ir, irregularity grade 1; Ir/P, irregular and pruned; FS, focal vasoconstriction/vasodilation grade 2–3; FS/P, focal vasoconstriction/vasodilation and pruned.

### Conventional Angiography in PRES

Vasculopathy was identified in 8 of 9 patients with CA demonstrating focal vasoconstriction, focal vasodilation, a string-of-bead appearance in at least 1 major arterial territory, or all 3 of these features. Involvement was most commonly in the second- and third-order branches but was also identified in fourth-order vessels and was frequently associated with regions of PRES vasogenic edema. Delay or reduced capillary blush was noted in all 9 patients (typically interhemispheric region, parietal-occipital lobes, or in areas of PRES vasogenic edema).

MRA was available in 6 of 9 patients with CA. In 3 of 6 patients, severe vessel irregularity consistent with vasculopathy (grade 2–3) was present on MRA and corresponded to the CA findings (Figs 1–3). In one of these patients (Fig 3), follow-up MRA demonstrated reversal of diffuse and focal vasoconstriction and vasodilation with worsening noted in the second patient.

In the other 3 patients, initial MRA demonstrated moderate to severe vessel irregularity and diffuse vasoconstriction, with follow-up CA demonstrating partial reversal with subtle residual vasculopathy in 2 and delayed or reduced interhemispheric capillary blush in 1.

### MRA in PRES

MRA was obtained in the immediate toxicity period (0–3 days) in 40 patients and at 4, 8, and 10 days after development of PRES in 3. Follow-up MRA was available in 11 of 43 patients.

### MRA with Follow-Up

In 7 of 11 patients, follow-up MRA demonstrated reversal of diffuse vasoconstriction with a distinct, and often marked, increase in vessel size and diameter along with improved visualization of the distal branch (On-line Table 1). Improved distal PCA visualization *only* was noted in 2 patients, and in 2 patients (each studied again at 4 days), follow-up MRA demonstrated worsening vessel irregularity and reduced branch visualization.

In patients demonstrating improvement, complete or near-complete normalization of vessel irregularity and vasculopathy was identified in 5 (follow-up imaging at 3, 11, 30, 90, and 162 days; Fig 3), improvement but still-obvious vessel irregularity in 3 (follow-up imaging at 2, 3, and 4 days), and significantly improved distal PCA visualization with improved, but persistent, vessel irregularity in 1 patient with sickle cell disease followed up at 33 days.

### Overall MRA and CA Observations

At MRA, diffuse vasoconstriction and focal vasculopathy were more frequently noted in patients with moderate to severe hypertension with vessel pruning, mild irregularity, or healthy appearance noted in patients who were normotensive (Table 3 and On-line Table 1 and Figs 1B, 2C, 3B, 3E, 4B, and 5B). Focal vasoconstriction (grade 2–3) was present at MRA in 30 of 43 patients and varied in each of the major branches (ACA [16 patients], MCA [18 patients], and PCA [23 patients]).

Overall, in 40 (87%) of 46 patients, MRA and CA results demonstrated vessel abnormality consistent with diffuse vasoconstriction, focal vasculopathy (grade 2–3), or vessel pruning. First-order branch spasm was identified in 5 patients with possible mild first-order spasm in an additional 6 patients. Second- and third-order focal branch spasm was identified by CA and MRA in 33 of 46 patients.

### MRA and Vasogenic Edema Comparison in Patients Who Were Severely Hypertensive

Extent of PCA pruning relative to the extent of hemispheric edema was compared in the patients who were severely hypertensive and are summarized in Table 4. Vasogenic edema was less in patients who demonstrated lengthy visualization of the PCA and calcarine artery (Fig 5) with more severe edema in those patients with moderate to severe PCA pruning (Fig 4).

Therefore, hemispheric edema trended downward with greater visualized length of the PCA and calcarine arteries, which was statistically significant ( $P = .002$ ). The observation remained statistically significant when only the 25 patients imaged within 1 day of toxicity ( $P = .003$ ) were considered. No statistically significant difference was detected in the PCA grade relative to the timing of the MR image from recognized neurotoxicity. Interobserver agreement of the PCA grade was 86% before consensus resolution.

### MRP in PRES

In 15 of 20 patients, the MRP studies were of good quality, and reliable measurements of rCBV could be made with 5 studies not evaluated because of an irregular bolus or motion artifact. There were 70 abnormal-appearing lesions or regions present in the 15 patients, with reliable rCBV measurements made in 59 of these 70 locations (On-line Table 2 and Fig 6).

In 51 (86%) of 59 PRES lesions and regions, rCBV was markedly diminished ( $\leq 80\%$ ; average,  $61\% \pm 12\%$ ; range, 31%–80%) compared with the healthy reference cortex. In 8 studied lesions, rCBV was between 84% and 99% of the healthy cortex rCBV (single lesion in 5 patients, 3 lesions in 1 patient studied 3 days after toxicity). Overall average rCBV in all measured PRES lesions and regions relative to a reference normal cortex rCBV was  $65.2\% \pm 14.8\%$  (range, 31%–99%).

### Discussion

The cause of PRES is not established. Classically, neurotoxicity with PRES is associated with cyclosporine and FK-506 (transplantation), preeclampsia and eclampsia, autoimmune disease, and postchemotherapy.<sup>1–12,24</sup>

The mechanism of PRES remains controversial. Severe hypertension with autoregulatory failure and forced hyperperfusion remains widely accepted. Alternatively, vasospasm is reported (MRA or CA), and reduced perfusion has been



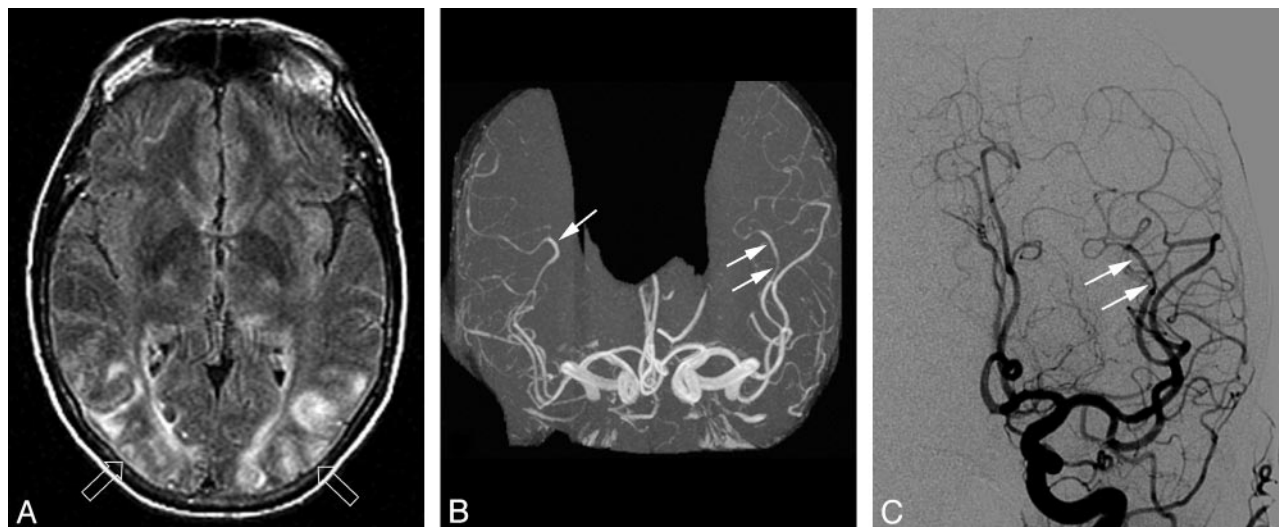


**Fig 1.** Patient 43 is a 53-year-old woman with a baseline blood pressure of 131/74 mm Hg who was receiving oral and skin patch narcotic pain control for a recently sustained pelvic fracture in a motor vehicle crash. She developed nausea, vomiting, and altered mentation then progressed to generalized seizure with a blood pressure at toxicity of 149/105 mm Hg. *A*, Axial MR imaging (FLAIR sequence) obtained 1 day after acute toxicity demonstrates vasogenic edema in the occipital region (*open arrows*) consistent with PRES. Similar areas of vasogenic edema consistent with PRES was present in the frontal and parietal regions (*not shown*). *B*, MR angiogram obtained on the same day demonstrates areas of focal vasodilation in the branches of MCA bilaterally with focal vasoconstriction also noted on the left (*arrows*). *C*, Frontal view from the left common carotid catheter angiogram obtained the same day demonstrates an identical area of focal vasodilation and vasoconstriction in the branch of the left MCA (*arrow*). An identical finding was present at angiography in the right MCA consistent with the MRA observation on the right. Similar findings were present on both MRA and CA in the PCA bilaterally (*not shown*).

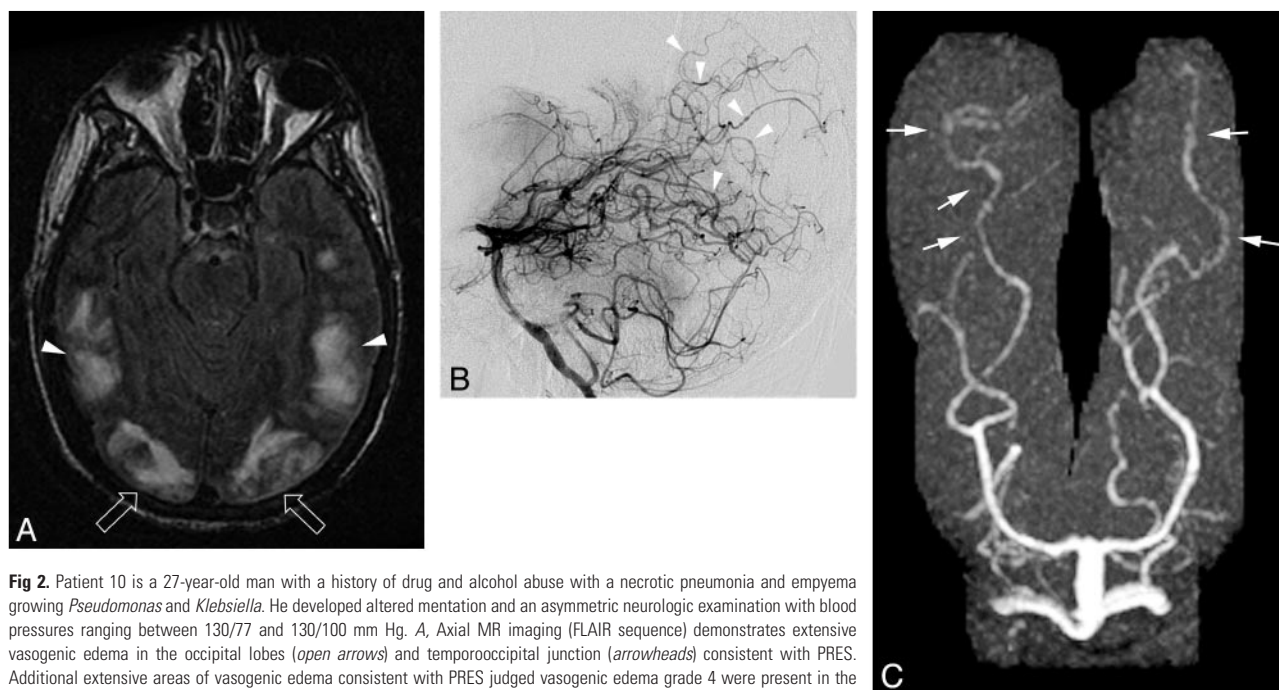


**Fig 2.** Patient 10 is a 27-year-old man with a history of drug and alcohol abuse with a necrotic pneumonia and empyema growing *Pseudomonas* and *Klebsiella*. He developed altered mentation and an asymmetric neurologic examination with blood pressures ranging between 130/77 and 130/100 mm Hg. *A*, Axial MR imaging (FLAIR sequence) demonstrates extensive vasogenic edema in the occipital lobes (*open arrows*) and temporooccipital junction (*arrowheads*) consistent with PRES. Additional extensive areas of vasogenic edema consistent with PRES judged vasogenic edema grade 4 were present in the frontal and parietal lobes (*not shown*). *B*, Vertebral catheter angiogram obtained after development of occipital hemorrhage (5 days after initial toxicity) demonstrates areas of vessel narrowing and dilation along with a string-of-bead appearance and areas of focal spasm in parietal and occipital branches of the PCA. Right common carotid catheter angiogram (*not shown*) also demonstrated extensive vasospasm in branches of the ACA and MCA. *C*, MR angiogram obtained 5 days after catheter angiogram (10 days after initial toxicity) demonstrates persistent vessel irregularity in the posterior cerebral branches (*arrows*) with a pattern nearly identical to the appearance of the catheter angiogram. Follow-up MR imaging demonstrated improvement of the extensive vasogenic edema.

demonstrated (MRP, technetium Tc99m hexamethylpropyleneamine oxime single-photon emission CT with a watershed lesion distribution suggesting hypoperfusion.<sup>1-3,5,9,13-20</sup>

The autoregulatory response is intended to maintain stable cerebral blood flow in the face of blood pressure fluctuations.<sup>25,26</sup> With acute severe hypertension, precapillary arteriolar vasoconstriction occurs in small (30–300  $\mu$ ) resistance vessels that limit cerebral blood flow (upper-limit-of-response

MAP, 140–160 mm Hg in patients who are normotensive).<sup>25-29</sup> This seems to be regulated by the endothelium through effects of elevated transmural pressure and release of thromboxane A2 and endothelin.<sup>26</sup> The upper limit is increased in the setting of essential hypertension and sympathetic stimulation as may exist in patients with cyclosporine toxicity.<sup>25,27</sup> Above this upper-threshold MAP, passive vasodilation ensues with subsequent increase in CBF and endothe-

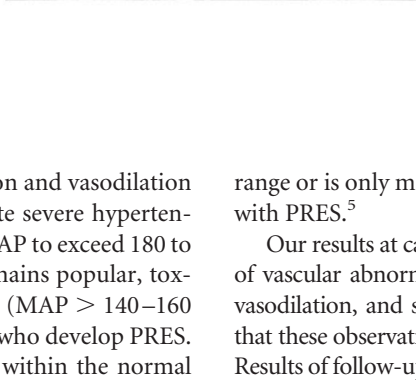
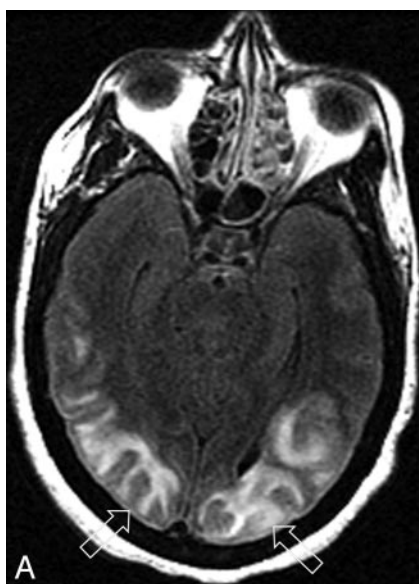
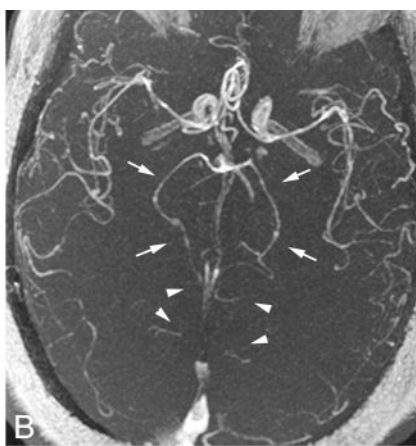
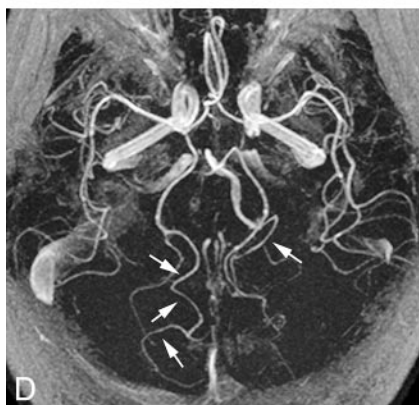
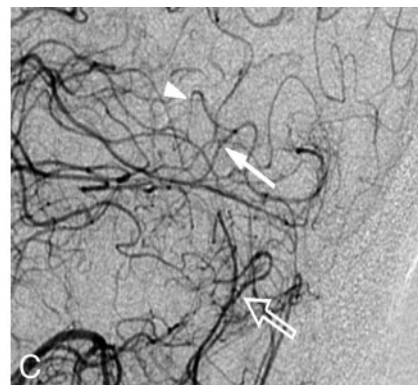
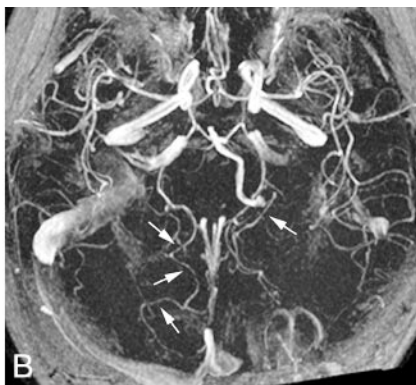
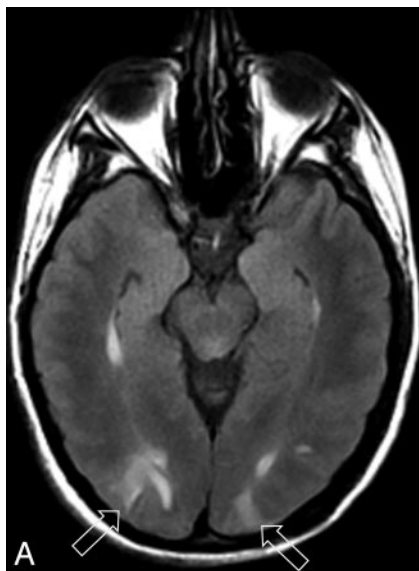


**Fig 3.** Patient 16 is a 39-year-old woman status post bowel resection and appendectomy for Crohn disease being maintained on antibiotics and steroids with baseline blood pressure of 100/60 mm Hg. Brain imaging was obtained when she developed headache, vertigo, and moderate elevation in blood pressure (145/95 mm Hg). **A**, Axial MR imaging (FLAIR sequence) results demonstrate vasogenic edema in occipital lobes (open arrows) consistent with PRES. Additional areas of vasogenic edema consistent with PRES were present in the frontal and parietal regions, and abnormality of signal intensity with restricted diffusion was also present in the medial right cerebellar hemisphere (not shown). **B**, MR angiogram obtained 1 day after toxicity demonstrates marked vessel irregularity in the PCAs bilaterally (arrows), greater on the right than on the left. **C**, Left vertebral catheter angiogram (selected posterior magnified lateral view) demonstrates a beaded appearance (arrow) and focal vasoconstriction and vasodilation (arrowhead) of right third- and fourth-order branches of the PCA along with a beaded appearance of the branches of the distal medial posterior inferior cerebellar artery on the left (open arrow). **D** Results of follow-up MR angiogram obtained 3 days after initial study demonstrate normalization of the vessel irregularity and marked improvement in vessel caliber (arrows) consistent with reversal of the vasospasm/arteritis confirmed on conventional angiography. Follow-up MR imaging demonstrated reversal of the PRES pattern.

**Fig 4.** Patient 34 is a 56-year-old woman with long-standing sickle cell disease and a baseline blood pressure of 140/60 mm Hg in a sickle cell crisis with new-onset pneumonia. She developed altered mental status and a seizure with blood pressure at toxicity of 170/110 mm Hg. **A**, Axial MR imaging (FLAIR sequence) demonstrates typical vasogenic edema in the occipital pole regions bilaterally (open arrows) consistent with PRES and judged edema, grade 3. Occipital lobe rCBV relative to a healthy reference cortex was 63% on the right and 54% on the left. **B**, Collapsed view of the 3D TOF MRA sequence demonstrates both focal vasospasm (arrows) and pruning of the PCAs bilaterally. Foreshortening of the PCAs and only partial visualization to the midportion of the calcarine arteries are noted bilaterally (arrowheads) and were judged PCA pruning, grade 2. Follow-up MR imaging and MRA (not shown) obtained 1 month after toxicity demonstrated complete resolution of the vasogenic edema in the occipital poles with marked improvement in distal PCA flow bilaterally along with reversal of the pruning and vasospasm.

lial fluid transudation.<sup>26,27</sup> Vasoconstriction and vasodilation have been noted in animal studies of acute severe hypertension, but these changes typically require MAP to exceed 180 to 200 mm Hg.<sup>28,29</sup> Although this theory remains popular, toxicity MAP is identified at this critical level (MAP > 140–160 mm Hg) in only a small subset of patients who develop PRES. In addition, blood pressure at toxicity is within the normal

range or is only minimally elevated in 20% to 30% of patients with PRES.<sup>5</sup>

Our results at catheter angiography confirm a high incidence of vascular abnormality in PRES (focal vasoconstriction, focal vasodilation, and string-of-bead appearance) and demonstrate that these observations are reflected in the pattern seen at MRA. Results of follow-up MRA demonstrated reversibility of this vas-



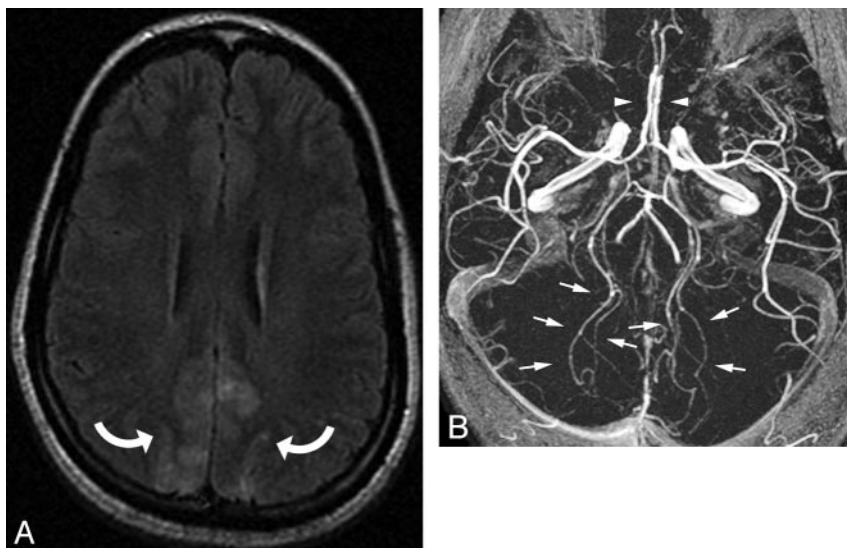


**Fig 5.** Patient 33 is a 23-year-old pregnant woman with baseline blood pressure of 125/75 mm Hg who developed eclampsia. Blood pressure at toxicity was 200/103 mm Hg. *A*, Axial MR imaging (FLAIR sequence) demonstrates vasogenic edema consistent with PRES in the parietal lobes bilaterally (curved arrows) and was judged edema, grade 1. Vasogenic edema consistent with PRES was also present in the frontal lobes, occipital region, and cerebellum (not shown). *B*, Collapsed view of the 3D TOF MRA sequence demonstrates PCA spasms bilaterally without PCA foreshortening (arrows) and was judged PCA pruning, grade 1. The ACA spasm present is also partially visible on this collapsed view (arrowheads).

**Table 4: Correlation of MRA pruning grade (PCA-calcarine artery) vs vasogenic edema: 28 patients with severe hypertension (MAP-136)**

Vasogenic Edema	PCA/Calcarine Artery Pruning Grade		
	Grade 1	Grade 2	Grade 3
Grade 4	0	1	1
Grade 3	3	1	0
Grade 2	6	4	0
Grade 1	12	0	0

**Note:**—MRA indicates magnetic resonance angiography; PCA, posterior cerebral artery; MAP, mean arterial pressure.

culopathy with normalization of diffuse vasoconstriction, reversal of focal vessel irregularity, and reduced vessel pruning consistent with previous reports.<sup>13,14</sup> In addition, MRP results demonstrated significantly reduced rCBV in most regions of PRES imaging abnormality compared with a reference healthy cortex. The observations in our patients are consistent with the vasculopathy and hypoperfusion in PRES.

In most of our patients, PRES developed after transplantation (cyclosporine and FK-506), infection, sepsis, shock, and eclampsia, all associated with systemic inflammation, endothelial activation and injury (upregulation of E-selectin, P-selectin, and intercellular adhesion molecule), and significant release of cytokines (tumor necrosis factor- $\alpha$  [TNF- $\alpha$ ] and interleukin-1 [IL-1]).<sup>30-35</sup> Endothelial activation and injury could independently inhibit flow or promote increased white cell and platelet adherence with subsequent blood flow effects at the capillary or venule level.<sup>36,37</sup> TNF- $\alpha$  and IL-1 promote endothelin-1 production and platelet degranulation could affect vessel tone, resulting in vasoconstriction.<sup>38,39</sup> These conditions also develop endothelial injury with hemolysis (red cell fragmentation, increased lactate dehydrogenase), capillary leakage with peripheral edema, and organ hypoperfusion. Vascular instability is common in preeclampsia, eclampsia, sepsis, and shock with both vasoconstrictive effects (platelet degranulation with thromboxane release, endothelin-1, angiotensin, vasopressin, and central sympathetic stimulation) and vasodilatory effects (nitric oxide, prostacyclin) noted.<sup>30,31</sup>

Brain vasculature may be experiencing a similar alteration

that is considered responsible for the systemic effects that lead to organ hypoperfusion in these conditions (endothelial activation, white cell trafficking, cerebral vasoconstriction). In the setting of significant hypoxemia, endothelial cells become activated and vascular endothelial growth factor mRNA (vascular endothelial growth factor (VEGF), previously known as vascular permeability factor) can upregulate with increased tissue levels of VEGF within 6 to 24 hours.<sup>40</sup> Sustained hypoperfusion and hypoxemia could result in expression of VEGF leading to endothelial leakage and vasogenic edema in PRES.

The features of vasoconstriction and vasodilation were identified in medium and small arteries ( $>300\ \mu$ ) even in the absence of significant hypertension. Vessel imaging appearance at CA and MRA might be reflecting the combined effects of both increased vessel tone (diffuse and focal vasoconstriction) and decreased tone (focal vasodilation) as can occur with induced endothelial injury or dysfunction.<sup>26</sup> PRES also occurred in patients with autoimmune diseases (ie, systemic lupus erythematosus), conditions with a known tendency to develop what is traditionally labeled arteritis.

Although only a small portion of our patients with PRES were studied with MRP, measurements of rCBV parallel results of other studies. In 51 (86%) measured lesions, rCBV was significantly reduced (average, 61%) compared with a healthy cortex. This is consistent with a case reported by Engelter et al<sup>19</sup> in which a rCBV lesion was 69% compared with healthy white matter). Brubaker et al<sup>20</sup> reports a somewhat lower average rCBV (28%) comparing the affected posterior part with the unaffected anterior part of the brain. This difference might be related to differing methodology or relatively small numbers of patients in both of our study groups.

Pruning and tapering of the PCA seems distinct from the observation of diffuse constriction and focal spasm of the PCA, though overlap was noted in many of our patients. Resistance to organ flow is primarily at the arteriole, capillary, or venule. If vasculopathy is present and resistance to brain blood flow is increased, arterial flow velocity will likely decrease with reduced vessel visualization on the 3D TOF MRA sequence. This could explain the pruned and tapered appearance.

Although severe vessel irregularity noted at MRA may appear nonspecific, these features, at least in part, reflect vascu-



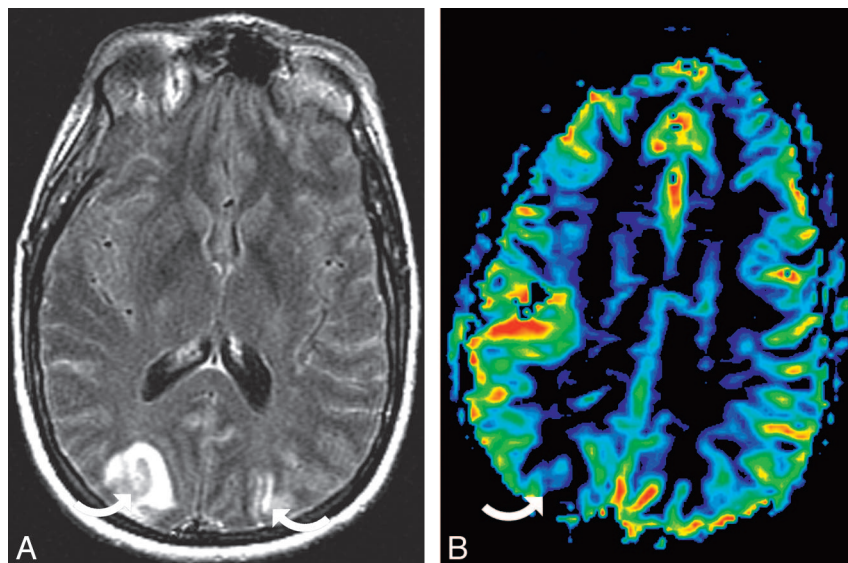


**Fig 6.** Patient 41 is a 34-year-old woman with baseline blood pressure of 104/60 mm Hg who at 33 weeks of pregnancy developed preeclampsia (toxicity blood pressure of 153/102 mm Hg) followed by seizures and status epilepticus. She ultimately required cesarean delivery for seizure control. **A**, Axial MR imaging (FLAIR sequence) demonstrates typical PRES vasogenic edema in the parietal regions (curved arrows) bilaterally and was judged edema, grade 2. Frontal and occipital involvement was also present bilaterally (not shown). **B**, rCBV color map demonstrates decreased perfusion in the region of the right parietal lesion (curved arrow). Lesion rCBV was 65% relative to a reference healthy cortex.

lopathy by their confirmation on CA and reversal as documented on follow-up MRA studies. Reduced cerebral blood flow as suggested by rCBV could further contribute to perceived vessel irregularity on the flow-sensitive 3D TOF MRA sequence. More widespread use of advanced technology such as 3T MR imaging and intracranial MRA performed during contrast infusion could markedly improve vessel margin visualization, reduce flow-related effects, and help augment detection of these subtle but important vascular features.

### **PRES and Hypertension**

PRES developing and spontaneously reversing in patients who are normotensive suggests a mechanism other than hypertension for the development of vasogenic edema. As graded in our study, vasogenic edema in patients with moderate and severe hypertension was not greater but actually was reduced compared with patients who were normotensive ( $P = .045$  between patients who were normotensive and those who were severely hypertensive). Most patients who were severely hypertensive demonstrated long-segment visualization of the PCA (despite diffuse vasoconstriction and focal spasm), and in these patients, more lengthy visualization of the PCA (PCA pruning grade 1) was associated with reduced brain edema ( $P = .002$ ). If failed autoregulation with passive vasodilation and hyperperfusion were the mechanism in PRES (with or without endothelial injury), one would expect the opposite observations including 1) a greater degree of edema in the severe hypertensive group compared with the normotensive group (accompanied by long-segment PCA visualization) and 2) a greater degree of vasogenic edema within the severe hypertensive group in those with greater PCA visualization.

Increased perfusion pressure might, at some point in the evolving systemic process, help maintain brain blood flow in the face of increased vascular resistance and hypoxemia, suggesting a protective effect. Elevated blood pressure and systemic vasoconstriction could be a reactive response (Cushing effect, biocontrol mechanism) designed to maintain adequate organ perfusion at the microvascular level. Of potential importance, severe *systemic* hypertension developing in the face of an increased state of vasoreactivity might augment cerebral

vasoconstriction (through autoregulation) and, like a biologic feedback loop, function to worsen hypoperfusion, endothelial dysfunction, or endothelial injury.

Several limitations of our study existed because of the retrospective nature of this evaluation. Standardized imaging timing and techniques (MRA, MRP, and brain imaging), computer modeling of vasogenic edema, broader clinical data recording (cytokines), and treatment may be of benefit. It is without doubt that a prospective assessment of PRES would be important.

### **Conclusion**

CA, MRA, and MRP demonstrate evidence of vasculopathy with focal and diffuse vasoconstriction, focal vasodilation, and a string-of-bead pattern along with reduced rCBV suggesting a state of brain hypoperfusion in PRES. Vasogenic edema was lower in patients who were hypertensive compared with those who were normotensive ( $P < .05$ ). In the patients who were severely hypertensive, better PCA visualization correlated with reduced vasogenic edema ( $P = .002$ ).

These features suggest that the primary abnormality in PRES could be related to reduced cerebral blood flow and that hypertension may, at some level, exert a protective effect limiting the developing of PRES and improving compromised cerebral perfusion.

### **Acknowledgments**

The authors thank Marcia Kurs-Lasky, MS, for her support with statistical analysis and Eric Jablonowski for his assistance with image preparation.

### **References**

1. Raroque HG, Orrison WW, Rosenberg GA. Neurologic involvement in toxemia of pregnancy: reversible MRI lesions. *Neuroradiology* 1990;40:167–69
2. Truwit CL, Denaro CP, Lake JR, et al. MR imaging of reversible cyclosporin A-induced neurotoxicity. *AJNR Am J Neuroradiol* 1991;12:651–59
3. Bartynski WS, Grabb BC, Zeigler Z, et al. Watershed imaging features and clinical vascular injury in cyclosporin A neurotoxicity. *J Comput Assist Tomogr* 1997;21:872–80
4. Schaefer PW, Buonanno FS, Gonzalez RG, et al. Diffusion-weighted imaging

- discriminates between cytotoxic and vasogenic edema in a patient with eclampsia. *Stroke* 1997;28:1082–85
5. Bartynski WS, Zeigler Z, Spearman MP, et al. Etiology of cortical and white matter lesions in cyclosporin-A and FK-506 neurotoxicity. *AJNR Am J Neuroradiol* 2001;22:1901–14
  6. Hinchey J, Chaves C, Appignani B, et al. A reversible posterior leukoencephalopathy syndrome. *N Engl J Med* 1996;334:494–500
  7. Provenzale JM, Petrella JR, Cruz LC, et al. Quantitative assessment of diffusion abnormalities in posterior reversible encephalopathy syndrome. *AJNR Am J Neuroradiol* 2001;22:1455–61
  8. Covarrubias DJ, Leutner PH, Campeau NG. Posterior reversible encephalopathy syndrome: prognostic utility of quantitative diffusion-weighted MR images. *AJNR Am J Neuroradiol* 2002;23:1038–48
  9. Rippe DJ, Edwards MK, Schrodt JF, et al. Reversible cerebral lesions associated with tiazofurin usage: MR demonstration. *J Comput Assist Tomogr* 1988;12:1078–81
  10. Vaughn DJ, Jarvik JG, Hackney D, et al. High-dose cytarabine neurotoxicity: MR findings during the acute phase. *AJNR Am J Neuroradiol* 1993;14:1014–16
  11. Ito Y, Arahata Y, Goto Y, et al. Cisplatin neurotoxicity presenting as reversible posterior leukoencephalopathy syndrome. *AJNR Am J Neuroradiol* 1998;19:415–17
  12. Bartynski WS, Zeigler ZR, Shaddock RK, et al. Pretransplantation conditioning influence on the incidence of cyclosporine or FK-506 neurotoxicity in allogeneic bone marrow transplantation. *AJNR Am J Neuroradiol* 2004;25:261–69
  13. Bartynski WS, Boardman JF, Zeigler ZR, et al. Posterior reversible encephalopathy syndrome in infection, sepsis, and shock. *AJNR Am J Neuroradiol* 2006;27:2179–90
  14. Lin JT, Wang SJ, Fuh JL, et al. Prolonged reversible vasospasm in cyclosporin A-induced encephalopathy. *AJNR Am J Neuroradiol* 2003;24:102–04
  15. Ito T, Sakai T, Inagawa S, et al. MR angiography of cerebral vasospasm in preeclampsia. *AJNR Am J Neuroradiol* 1995;16:1344–46
  16. Sengar AR, Gupta RK, Dhanuka AK, et al. MR imaging, MR angiography, and MR spectroscopy of the brain in eclampsia. *AJNR Am J Neuroradiol* 1997;18:1485–90
  17. Bartynski WS, Sanghvi A. Neuroimaging of delayed eclampsia. Report of 3 cases and review of the literature. *J Comput Assist Tomogr* 2003;27:699–713
  18. Naidu K, Moodley J, Corr P, et al. Single photon emission and cerebral computerised tomographic scan and transcranial Doppler sonographic findings in eclampsia. *Br J Obstet Gynaecol* 1997;104:1165–72
  19. Engelter ST, Petrella JR, Alberts MJ, et al. Assessment of cerebral microcirculation in a patient with hypertensive encephalopathy using MR perfusion imaging. *AJR Am J Roentgenol* 1999;173:1491–93
  20. Brubaker LM, Smith JK, Lee YZ, et al. Hemodynamic and permeability changes in posterior reversible encephalopathy syndrome measured by dynamic susceptibility perfusion-weighted MR imaging. *AJNR Am J Neuroradiol* 2005;26:825–30
  21. Ferris EJ. Arteritis. In: Newton TH, Potts DG. *Radiology of the skull and brain: Angiography*. Reprinted by Great Neck, New York: MediBooks, 1986; original printing by Mosby 1974:2566–97
  22. Osborne A. Nonatheromatous vasculopathy. In: Osborne A. *Diagnostic cerebral angiography*, 2nd ed. Philadelphia: Lippincott Williams and Wilkins; 1999:341–58
  23. Agresti A, Mehta CR, Patel NR. Exact inference for contingency tables with ordered categories. *J Am Stat Assoc* 1990;85:453–58
  24. Gijtenbeek JM, van den Bent MJ, Vecht CJ. Cyclosporine neurotoxicity: a review. *J Neurol* 1999;246:339–46
  25. Cerebral blood flow, cerebrospinal fluid, and brain metabolism. In: Guyton AC, Hall JE. *Textbook of medical physiology*. Philadelphia: Elsevier; 2006:761–68
  26. Zwienenberg-Lee M, Muizelaar JP. Clinical pathophysiology of traumatic brain injury. In: Winn HR, ed. *Youmans neurological surgery*, 5th ed. Philadelphia: Saunders; 2004:5039–63
  27. Busija DW, Heistad DD, Marcus ML. Effects of sympathetic nerves on cerebral vessels during acute, moderate increases in arterial pressure in dogs and cats. *Circ Res* 1980;46:696–702
  28. Kontos HA, Wei EP, Navari RM, et al. Responses of cerebral arteries and arterioles to acute hypotension and hypertension. *Am J Physiol* 1978;234:H371–83
  29. MacKenzie ET, Strandgaard S, Graham DI, et al. Effects of acutely induced hypertension in cats on pial arteriolar caliber, local cerebral blood flow, and the blood brain barrier. *Circ Res* 1976;39:33–41
  30. Cunningham FG, Gant NF, Leveno KJ, et al. Hypertensive disorders in pregnancy. In: Cunningham FG, Gant NF, Leveno KJ, et al, eds. *Williams Obstetrics*, 21st ed. 2001:567–618
  31. Munford RS. Sepsis, severe sepsis, and septic shock. In: Mandell GL, Bennett JE, Dolin R, eds. *Principles and practice of infectious disease*. Philadelphia: Elsevier; 2005:906–26
  32. Ferrara JL. Pathogenesis of acute graft-versus-host disease: cytokines and cellular effectors. *J Hematother Stem Cell Res* 2000;9:299–306
  33. Schots R, Kaufman L, Van Riet I, et al. Proinflammatory cytokines and their role in the development of major transplant-related complications in the early phase after allogeneic bone marrow transplantation. *Leukemia* 2003;17:1150–56
  34. Bartynski WS, Zeigler ZR, Shaddock RK, et al. Variable incidence of cyclosporine and FK-506 neurotoxicity in hematopoietic malignancies and marrow conditions after allogeneic bone marrow transplantation. *Neurocrit Care* 2005;3:33–45
  35. Daly AS, Xenocostas A, Lipton JH. Transplantation-associated thrombotic microangiopathy: twenty-two years later. *Bone Marrow Transplant* 2002;30:709–15
  36. Parent C, Eichacker PQ. Neutrophil and endothelial cell interactions in sepsis. The role of adhesion molecules. *Infect Dis Clin North Am* 1999;13:427–47, x
  37. McCuskey RS, Urbaschek R, Urbaschek B. The microcirculation during endotoxemia. *Cardiovasc Res* 1996;752–63
  38. Wanecek M, Weitzberg E, Rudehill A, et al. The endothelin system in septic and endotoxin shock. *Eur J Pharmacol* 2000;407:1–15
  39. Mantovani A, Bussolino F, Dejana E. Cytokine regulation of endothelial cell function. *FASEB J* 1992;6:2591–99
  40. Schoch HJ, Fischer S, Marti HH. Hypoxia-induced vascular endothelial growth factor expression causes vascular leakage in the brain. *Brain* 2002;125:2549–57